Research Article | Vol. 10, No. 3 | 1 Mar 2019 | BIOMEDICAL OPTICS EXPRESS 1207
Biomedical Optics EXPRESS

Optical coherence tomography-guided laser marking with tethered capsule endomicroscopy in unsedated patients

CHIA-PIN LIANG,[1] JING DONG,[1] TIM FORD,[1] ROHITH REDDY,[1] HAMID HOSSEINY,[1] HAMID FARROKHI,[1] MATTHEW BEATTY,[1] KANWARPAL SINGH,[1] HANY OSMAN[1], BARRY VUONG,[1] GRACE BALDWIN,[1] CATRIONA GRANT,[1] SARAH GIDDINGS,[1] MICHALINA J. GORA,[1,2] MIREILLE ROSENBERG,[1] NORMAN NISHIOKA,[3] AND GUILLERMO TEARNEY[1,4,5,*]

[1]*Wellman Center for Photomedicine, Harvard Medical School and Massachusetts General Hospital, 55 Fruit Street, Boston, MA 02114, USA*
[2]*ICube Laboratory, CNRS, Strasbourg University, Strasbourg, France*
[3]*Department of Gastroenterology, Harvard Medical School and Massachusetts General Hospital, 55 Fruit Street, Boston, MA 02114, USA*
[4]*Harvard-MIT Division of Health Sciences and Technology, 77 Massachusetts Avenue, Cambridge, MA 02139, USA*
[5]*Department of Pathology, Harvard Medical School and Massachusetts General Hospital, 55 Fruit Street, Boston, MA 02114, USA*
**gtearney@partners.org*

Abstract: Tethered capsule endomicroscopy (TCE) is an emerging screening technology that comprehensively obtains microstructural OCT images of the gastrointestinal (GI) tract in unsedated patients. To advance clinical adoption of this imaging technique, it will be important to validate TCE images with co-localized histology, the current diagnostic gold standard. One method for co-localizing OCT images with histology is image-targeted laser marking, which has previously been implemented using a driveshaft-based, balloon OCT catheter, deployed during endoscopy. In this paper, we present a TCE device that scans and targets the imaging beam using a low-cost stepper motor that is integrated inside the capsule. In combination with a 4-laser-diode, high power 1430/1450 nm marking laser system (800 mW on the sample and 1s pulse duration), this technology generated clearly visible marks, with a spatial targeting accuracy of better than 0.5 mm. A laser safety study was done on swine esophagus *ex vivo*, showing that these exposure parameters did not alter the submucosa, with a large, 4-5x safety margin. The technology was demonstrated in living human subjects and shown to be effective for co-localizing OCT TCE images to biopsies obtained during subsequent endoscopy.

1. Introduction

Tethered capsule endomicroscopy (TCE) is a new technology that implements optical coherence tomography (OCT) using a swallowable capsule that can be administered in unsedated patients [1,2]. Once swallowed, the device traverses the gastrointestinal (GI) tract, continuously collecting OCT images, creating a three-dimensional microscopic map of the esophagus in its entirety [1,2]. The procedure takes only 5-6 minutes and patients can return to their daily activities immediately after it is over [3,4]. Multiple studies have demonstrated the promise of using TCE for screening for esophageal diseases in patients [1–7], for other upper GI tract organs [8], and the use of esophageal TCE has been reported in a primary care clinic [3]. As opposed to endoscopy, TCE does not require sedation or a specialized setting and can be conducted by nurses or technicians. Following the procedure, the device can be

#349331 https://doi.org/10.1364/BOE.10.001207
Journal © 2019 Received 26 Oct 2018; revised 23 Dec 2018; accepted 6 Jan 2019; published 12 Feb 2019

Biomedical Optics EXPRESS

disinfected and reused many times (> 10 times), driving per patient costs down. These features of OCT-TCE potentially make it useful for screening for diseases such as Barrett's Esophagus (BE), which heretofore has not been well addressed by upper endoscopy [9].

The next major step in the clinical translation of TCE for screening is the validation of its diagnostic accuracy against the gold standard, histopathology of endoscopically acquired biopsies. Requisite co-localization of OCT images and biopsies can be challenging using whole organ microscopy techniques such as balloon-based volumetric laser endomicroscopy (VLE) [10,11] and TCE. Using of the same catheter to deliver OCT light and the higher power laser light solves this issue by creating endoscopically-visible fiducial marks in the patient's esophagus that correspond to specific OCT targets [12,13]. Biopsies taken from these marked sites are inherently co-localized to the target OCT image within an uncertainty caused by patient/device motion that occurs between target selection and mark creation [12,13]. Studies using driveshaft-based, centering balloon VLE have shown that laser marking is highly effective for co-localizing esophageal OCT images with histology, with a spatial targeting error of about 1 mm. Balloon-based VLE targeting using laser marking is now being used clinically in multiple centers to good effect [13,14].

Laser marking in TCE devices has additional challenges, such as greater motion of the device in vivo, as it is not easily held in one place as opposed to the much larger diameter balloon. Our previous laser marking study in human subjects with TCE capsule (unpublished) showed that laser marks were irregular and ineffective when generated using a 2-second exposure duration (Fig. 1). The instability of the capsule in the esophagus necessitates that the time required to generate a laser mark be reduced from 2 s. We developed a new marking system that provided higher power to shorten the exposure time to 1 s to mitigate motion artifact.

In addition, it has been recognized that scanning the beam with a micromotor integrated into the capsule has many advantages over driveshaft mechanical scanning. One of the most important benefits of micromotor-based TCE is reduced non-uniform rotational distortion (NURD) artifacts [15] that can become especially severe when the subject bites on the tether. Here, we report the development, validation, and human use of an integrated stepper micromotor-based laser marking TCE device and system.

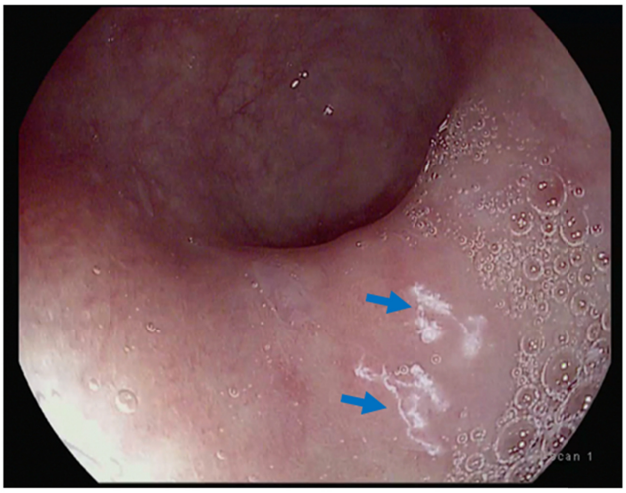

Fig. 1. Endoscopic image of TCE laser marking using a tissue irradiation power of 400 mW over a duration of 2 seconds. Blue arrows indicate the marking sites that are irregular and distorted due to tissue motion during the exposure period.

Biomedical Optics EXPRESS

2. Methods

2.1 Laser marking study in swine esophagus ex vivo

Our prior study in subjects (Fig. 1) showed that laser marks were irregular and ineffective when generated using a 2 seconds exposure duration. We then increased power to 800 mW and decreased the laser marking time to 1 second. We conducted a study in swine esophagus ex vivo to determine the anatomic cautery depth for the new parameters. The esophagus was excised from euthanized swine (Yorkshire, > 40 kg), cut open, and covered by a Poly(methyl methacrylate) (PMMA) sheet to mimic the capsule. A single-mode fiber ball lens probe, similar to that used in our TCE devices, was placed above the PMMA sheet, delivering laser energy onto the sample. The spot size measured at 1310 nm was 37 μm, which was consistent with the spot sizes of our typical TCE devices. The tissue was exposed with 800 mW, 1450 nm laser light through the core of the single mode fiber for 1s, 2s, 3s and 4s at 3 different locations along the esophagus (distal, mid, proximal). Immediately thereafter, tissue cryosection block was prepared and a 10-micron tissue cryosection was cut every 150 microns through the cautery sites. The sections were stained by nitro-blue tetrazolium chloride (NBTC) to differentiate thermally injured tissue from viable tissue. The maximum depth and lateral extent of each cautery spot was morphometrically measured. A total of 9 cautery sites (distal, mid and proximal sites from each animal, 3 animals in total) were analyzed for each exposure time. The mean thermal injury depths and lateral width were tabulated for the different exposure times. In addition, the distances between the maximum thermal injury depths and the superficial boundaries of the submucosa were measured. Statistical analysis using ANOVA was performed to investigate if different locations (proximal, mid and distal) created a different injury under the same laser exposure time. P values were calculated, and $p < 0.05$ criteria was used for determining whether difference was statistically significant.

2.2 In vivo clinical system

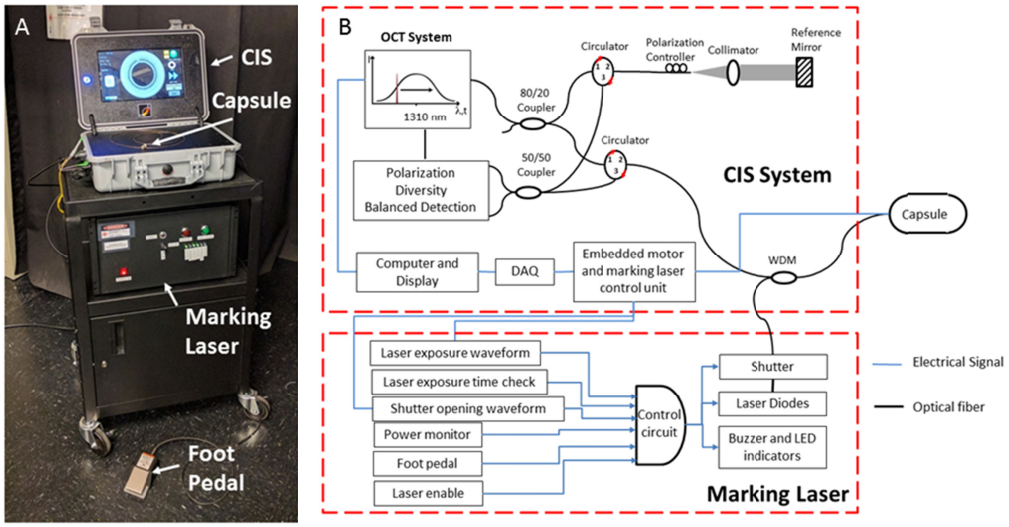

Fig. 2. (A) Photograph of the clinical compact imaging system (CIS) with marking laser system and TCE capsule. (B) Schematic of the clinical system.

A clinical OCT-guided marking laser system was built, tested and IRB approved (IRB 13-P001254, IRB 17-P001752) for subsequent in vivo human studies. The system consisted of a compact imaging system (CIS), a marking laser system and a tethered capsule (Fig. 2). The

Biomedical Optics EXPRESS

imaging system, containing an Axsun swept source laser, provided real-time (39 frames/s, 100 kHz A-line scan rate) microstructural OCT imaging for identifying the tissue targets. Once a target was identified, the operator could select the target on the OCT image by placing a finger on the image on the touch screen display. The coordinate of the target was sent to the embedded motor and marking laser control unit (Fig. 2(B)). After receiving the execution command, the control unit automatically stopped the motor in the capsule to aim the marking laser at the target, opened the shutter, and activated the marking laser. The marking laser light and OCT imaging light were coupled into the same single mode fiber in the TCE device through a wavelength division multiplexing (WDM) coupler.

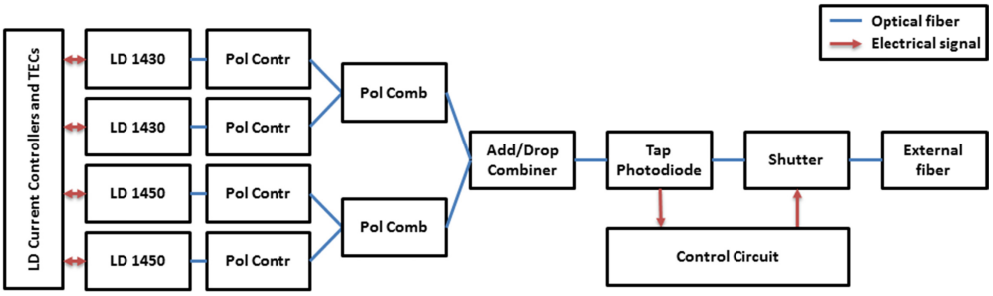

Fig. 3. Schematic of marking laser subcomponents.

To minimize tissue motion artifacts (Fig. 1), the exposure time was set at 1 s. This decrease in exposure time necessitates a laser power increase to maintain the total energy (0.8 J) that can create laser marks [12,16]. Given the commercially available single mode lasers that we identified and optical losses in the system and TCE device, we needed 4 laser diodes (Fig. 3) to achieve a total of 800 mW on the tissue. Polarization multiplexing was used for combining the power from the two diodes at the same wavelength with a given polarization state. Wavelength multiplexing using lasers at 1430 and 1450 nm wavelength was conducted to increase power further. Both laser wavelengths had good water absorption efficiency (extinction coefficients: 29.26 and 30.54 cm^-1 for 1430 nm and 1450 nm respectively), which is required for tissue marking. The power from the single mode laser diodes was coupled into a single mode fiber and transmitted through the same optics used for imaging. The power from the laser diode pair for each wavelength was efficiently combined by asserting cross-polarization states with polarization controllers (Pol Contr) and mixing with a polarization combiner (Pol Comb). Then, the laser light at 1430 nm was combined with the light at 1450 nm by an add/drop combiner.

Several safety features were implemented for this Class IV marking laser: A laser exposure time monitoring circuit (Fig. 2(B)) to ensure the exposure time is within 1 second; A power monitor (Fig. 2(B) and 3, Tap photodiode) to guarantee the laser power is under the IRB-approved power limit (0.82 W); Foot pedal and laser enable button for quickly closing the shutter and disenabling the laser; Buzzer and LEDs for indicating the laser status. With these safety features, the tissue was irradiated with the right power, proper timing, over the specified duration.

Biomedical Optics EXPRESS

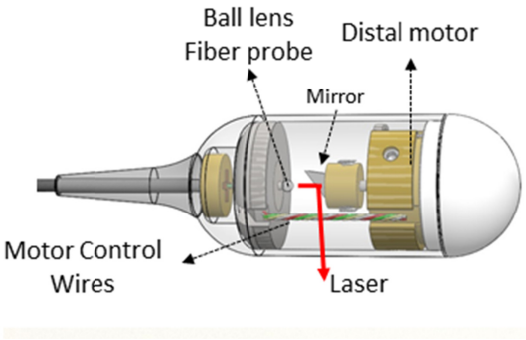

Fig. 4. Schematic of TCE capsule with a distal motor. The outer diameter of the capsule is 11 mm.

A distal 20-phase micro stepper motor was used within the capsule to scan the imaging beam and aim the marking laser at the target. Figure 4 shows the design of the TCE capsule with the distal micro stepper motor. OCT and marking light propagated through an optical fiber within the tether that was terminated by a ball lens fiber probe, producing a focal spot size of 30-40 µm. Light from the probe reflected off a mirror that was mounted on the motor's shaft to irradiate the tissue. 1310 nm OCT laser and 1430/1450 nm marking laser were focused at 0.59 mm and 0.8/0.82 mm from the capsule surface respectively. The outer diameter of the capsule is 11 mm. The electrical control signal was transmitted through the motor control wires to drive the motor.

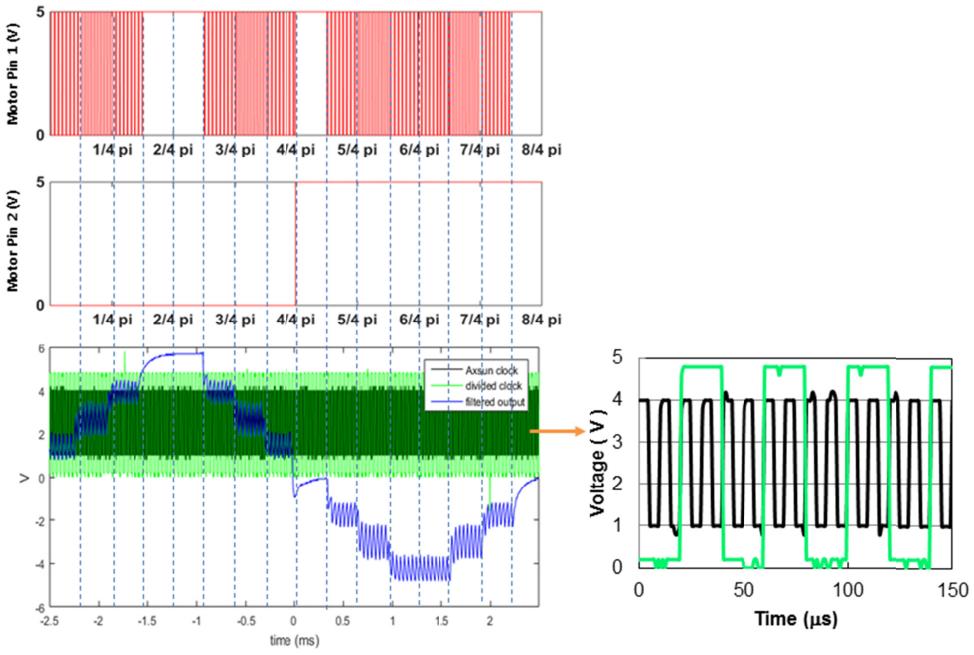

Fig. 5. Synchronized micro-stepping control signal for the distal stepper motor. The orange arrow indicates the zoom-in view of OCT engine and divided clock signal traces. V on vertical axis represents the voltage unit, volts.

A customized control scheme was implemented to perform encoder-free, high precision targeting (0.5 mm). To synchronize the motor's scan position with the image, the driving waveform was synchronized to the OCT A-line trigger (black trace in Fig. 5). After

Biomedical Optics EXPRESS

amplification and frequency division, the clock signal (green line) was fed into the microcontroller to generate a series of pulses (red lines). By changing the duty cycle (motor pin 1), subtracting the voltage with a reference pin (motor pin 2), and time averaging by the inductive electromagnetic winding, a sinusoid like motor driving waveform was generated (blue line). When the same driving waveform with a 90° phase shift was sent to the stepper motor's second winding, the rotor started to spin. The synchronization with the A-line clock stabilized the target in the imaging window, allowing the marking laser beam to be accurately directed to the target. Besides motor and imaging speed synchronization, the capability of performing micro-stepping was critical for high precision targeting. Once receiving the coordinate of target, the motor stopped at one of the dwelling points that was closest to the target. The maximum discrepancy between the intended position and the actual dwelling position was half of the space interval between two neighboring dwelling points. Without micro-stepping, the laser beam could only be stopped at 20 discrete positions along the 34.54 mm circumferential length of capsule, resulting in spatial resolution of 0.86 mm (half of the step size), which is too coarse for our application. Micro-stepping at 40 steps per rotation improves the theoretical targeting accuracy to 0.43 mm. We measured each step size and reported the histogram in the result section, section 3.2. While it was possible to introduce more than 40 steps to obtain better accuracy, a higher drive current would be required to maintain sufficient torque, potentially increasing the capsule's temperature to unsafe levels.

2.3 TCE laser marking clinical study

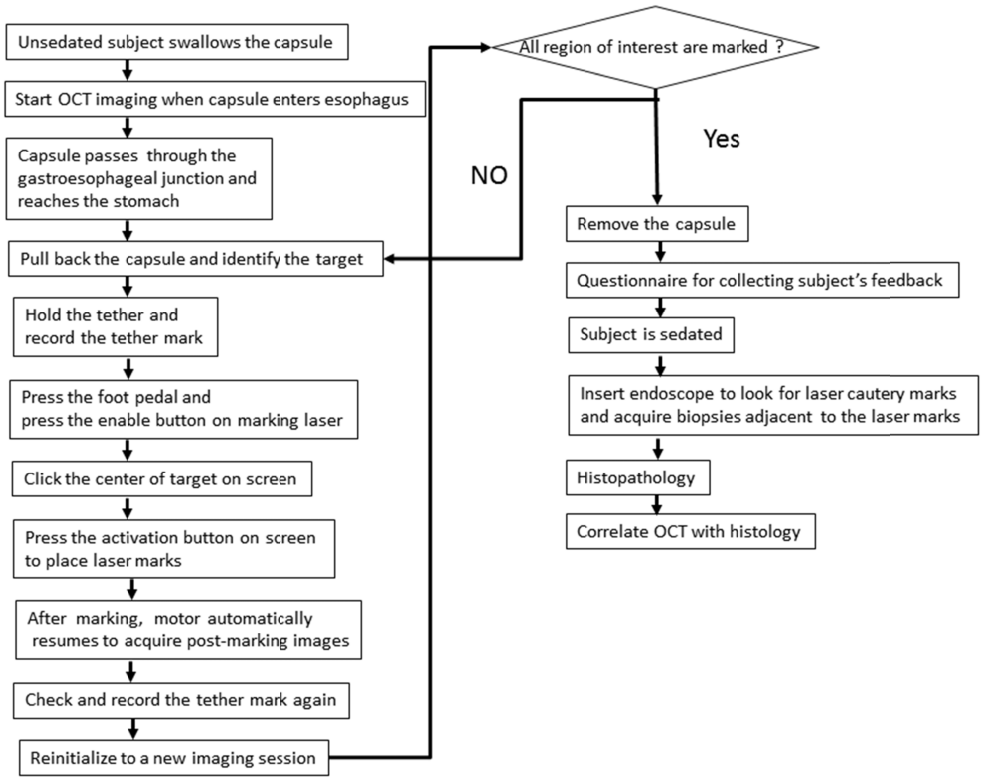

Fig. 6. Flow chart of the laser marking process used in the clinical study.

We are conducting a clinical study to test the laser marking TCE device. The study is approved by the Partners IRB (IRB 13-P001254, IRB 17-P001752) and a detailed protocol is listed on clinicaltrials.gov (https://clinicaltrials.gov/ct2/show/NCT02422433). Study subjects

Biomedical Optics EXPRESS

are recruited from patients with biopsy-proven BE, aged 18 and older, who are undergoing an upper endoscopy. After the capsule was swallowed by an unsedated subject, the operator started OCT imaging. Images were recorded while the capsule passively traveled down the esophagus. Once the OCT image indicated that the capsule had passed through the gastroesophageal junction and reached the stomach, the capsule was manually pulled back across the lower esophageal sphincter and through the esophagus using the tether. When a target of interest was identified during pull-back imaging, the tether was held in place, and the tether tick mark reading at the incisors was recorded. The operator subsequently stepped on the foot pedal and enabled the marking laser system by pressing the enable button. Then, the operator clicked on the target displayed on the screen and pressed the activation button to place the laser mark(s). One or two marks may be placed, depending on study protocols and user input prior to the procedure. After marking, the motor automatically resumed spinning to acquire post-marking images. Following a short period of post-marking imaging, the tether tick marks at the incisor were recorded again and imaging and pullback resumed. This process was repeated for the next region of interest (up to two marks per centimeter and a maximum of 6 marks per subject). Most laser markings were performed at the diseased area, which is typically at distal portion of the esophagus, near the gastroesophageal junction. After all targets in the subject were laser marked, the capsule was pulled out from the subject and a questionnaire regarding tolerability of the procedure was administered. Then, the subject was sedated and underwent standard of care endoscopy with biopsy. During the endoscopic procedure, the laser marks were identified and biopsies were acquired in between or adjacent to the laser marks. Histology from the biopsy samples were then correlated with the corresponding OCT images. When multiple biopsies were taken, the histology was further correlated with OCT data by the corresponding tether tick mark recorded at the incisors.

2.4 The targeting accuracy of TCE laser marking

We quantified the cross-sectional targeting accuracy in human subjects in vivo by subtracting the location of the selected target position in the pre-marking image from the location of hyper-reflective mark in the post-marking image. Pre- and post-marking images were first co-registered using anatomical landmarks (e.g. tissue fold, crypt, and glands etc.) shared by both images.

3. Results

3. 1 Laser thermal injury tests on ex vivo swine esophagus

Using 800 mW of power at 1430/1450 nm, the exposure time between 1 and 4 seconds created cauterized marks that were visually identifiable (Fig. 7(A)). Longer exposure times created larger cauterized marks. Figure 7(B) shows a representative NBTC histology image at a marking site (800 mW, 1s).

Biomedical Optics EXPRESS

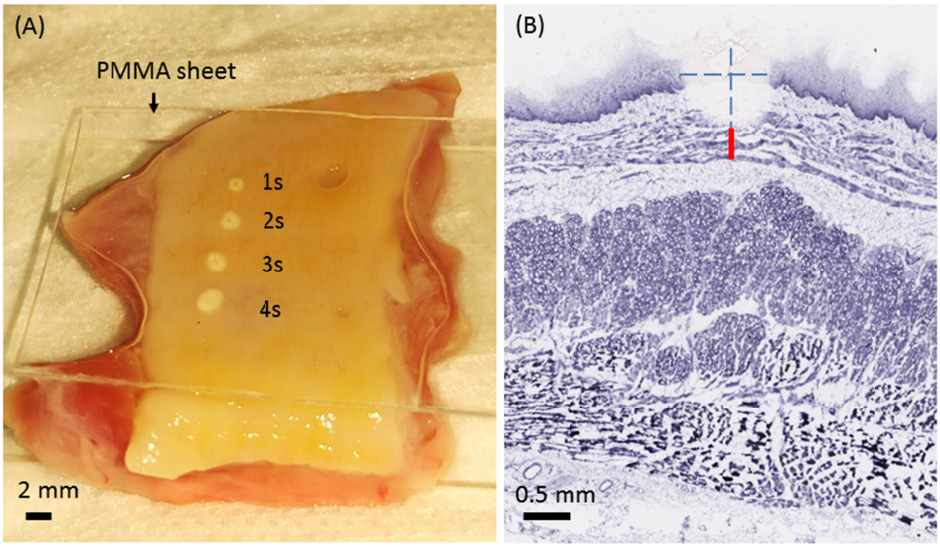

Fig. 7. (A) Photograph of marking sites on an excised swine esophagus lumen. Marks were generated with laser parameters of 1430/1450 nm, 800 mw, and 1-4 s exposure time. The illumination spot size was 37 μm. (B) A representative digitized NBTC-slide showing the mark obtained using 800 mw for 1s. The non-stained region delineates the extent of laser thermal injury. Blue dash lines indicate the injury width and depth. The red line indicates the distance between the deepest portion of the mark to the submucosa.

The dimensions of lateral and depth extent of the laser marks were measured (Fig. 7(B), blue dash lines) in addition to the distance between the deepest portion of the marks to the superficial boundary of the submucosal layer (Fig. 7(B), red line). Figure 8(A) shows that the lateral extent of the mark increased by approximately a factor of two between 1s and 4s. In contrast, the depth only increased by about 20% (Fig. 8(B)). The laser thermal injury did not penetrate beyond the muscularis mucosae even with a 4s exposure time (Fig. 8(C)). These findings demonstrate that 1430/1450 nm laser at 800 mW with 1-4 s exposure time produces defects in swine esophageal tissue that are comparable to the tissue removed by standard biopsy forceps. For the clinical study, we used a 1 s exposure time to minimize motion artifact.

Statistical analysis showed that there were no statistically significant differences in injury (lateral width, depth and the margin to the submucosa) between proximal, mid or distal locations ($p > 0.15$ for all 4 exposure durations).

Biomedical Optics EXPRESS

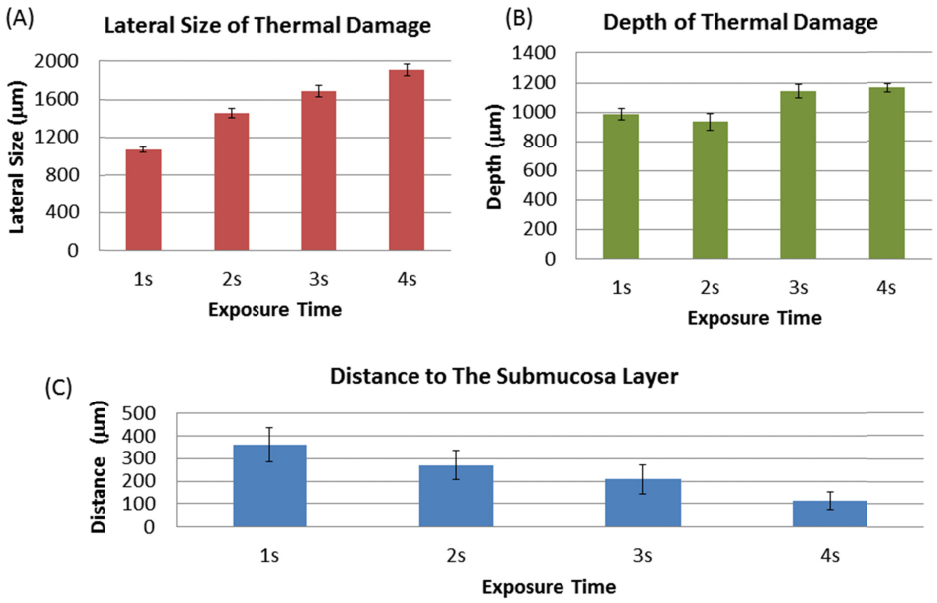

Fig. 8. Laser marking data from swine esophagus ex vivo using 800 mW of 1430/1450 nm light. The total number of data points for each exposure parameter is 9. Three data points (distal, middle and proximal esophagus) are collected from each of the three animals. (A) Bar chart of the lateral width of laser mark for different exposure times. (B) Bar chart of the depths of laser marks as a function for different exposure times. (C) Bar chart of distance between the deepest portion of the laser mark to the most superficial aspect of the submucosal layer for various exposure times. The error bars indicate standard error.

3.2 Performance of the TCE capsule with distal stepper motor

Figure 9 shows an image of a human esophagus, obtained *in vivo* with the micro-stepper motor TCE device. The distal stepper motor with the synchronized micro-stepping control generated high quality images *in vivo*.

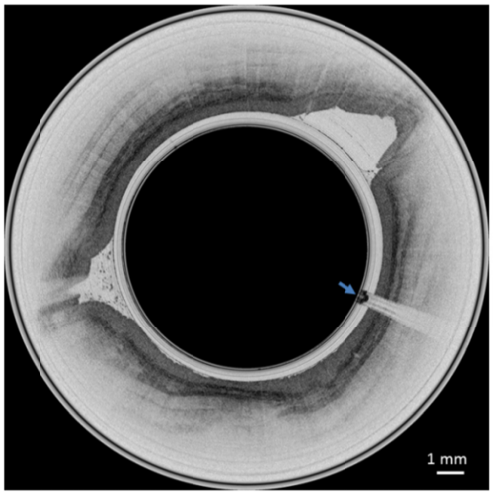

Fig. 9. An OCT image of human esophagus acquired by the TCE device with a distal stepper motor *in vivo*. The blue arrow demarcates the electrical wires that send the driving waveforms to the motor.

Biomedical Optics EXPRESS

Figure 10 shows the histogram of the increments of the beam around the outer surface of the capsule produced using a micro-stepping waveform comprising 40 steps. The average step size is 0.85 ± 0.09 mm (standard deviation). The maximum step size is 1 mm and thus the maximum error between the intended position and actual marking position is 0.5 mm.

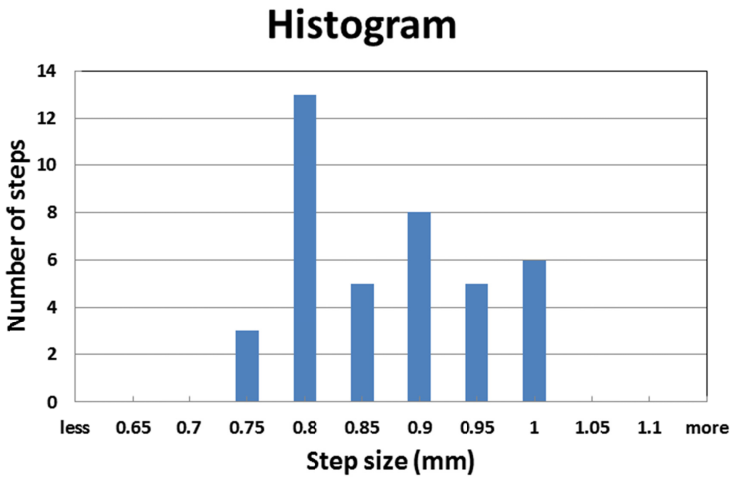

Fig. 10. Histogram of increments of the beam's position along the outer surface of the capsule when it is scanned using the micro-stepping motor (40 steps).

3.3 TCE laser marking clinical study

A total of 5 subjects (2 male / 3 female. Race: 5 white.) mean age 61.4 ± 5 (standard deviation) years old have undergone the TCE laser marking procedure. Two subjects were enrolled but excluded from the study. One excluded subject was unable to swallow the capsule. Another excluded subject had a previously undiagnosed candidiasis condition, which made it difficult to identify the laser marks endoscopically. The average time for the entire laser marking process was 7 ± 2 (standard deviation) minutes. The endoscopy procedure including sedation took 9.6 ± 3.6 (standard deviation) minutes and it took 38.4 ± 8.5 (standard deviation) minutes for the subjects to recover from the sedation. Laser marking was successful (laser mark placed that was visible on endoscopy) for 91.6% (11 out of 12 attempts) of the attempts. There were no cases where the patient sensed the mark when it was applied. There were also no complications of the TCE or laser marking procedure.

Figure 11 shows an example of TCE laser marking of a study subject's (a BE patient) esophageal squamous mucosa that is not involved with BE. The two red lines in the pre-marking OCT image (Fig. 11(A)) correspond to where the two laser marks are intended to be placed. These marks bracket the target tissue that has the typical layered appearance of esophageal squamous mucosa. The post-marking OCT image showed that the laser marks, seen as superficial hyperreflective regions, were placed where intended (Figs. 11(B) and (C), orange arrows). The laser marks were also clearly visible by conventional endoscopy performed after the TCE procedure, seen as white lesions on the surface of the esophagus (Fig. 11(D), red arrows). A biopsy was taken between the laser marks; histology (Fig. 11(E)) confirmed that the marked tissue contained normal esophageal squamous epithelium.

Biomedical Optics EXPRESS

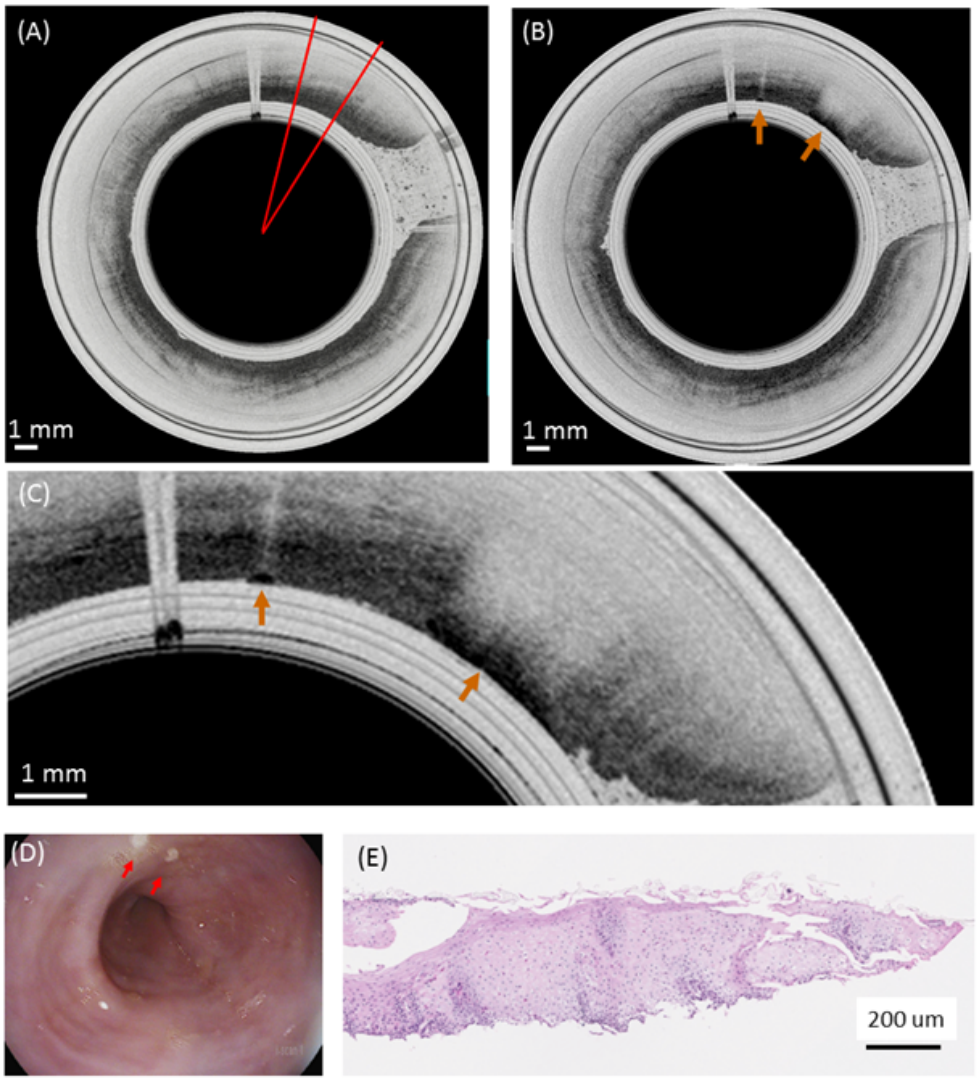

Fig. 11. TCE laser marking of a study subject's (a BE patient) normal esophagus. (A) Pre-marking OCT image of a region of the normal esophagus. The red lines indicate where the operator intends to place the laser marks. (B) OCT image of the study subject's esophagus after laser marking. Orange arrows demarcate the hyper-reflective signal from the cauterized laser marks. (C) Enlarged image of the marking sites, showing the OCT appearance of the laser marks (orange arrows) in greater detail. (D) Endoscopy image of the laser marks (red arrows). (E) Histology from a biopsy taken between the two laser marks confirms that the tissue between the marks is squamous epithelium.

Figure 12 shows an example of TCE laser marking guided biopsy of Barrett's esophagus, in vivo. The pre-marking OCT image (Fig. 12(A)) shows BE as tissue without squamous layering, heterogeneous backscattering, and an irregular mucosal surface. For this case, only one laser mark was applied on the BE region at the location denoted by the red line (Fig. 12(A)). After the laser mark was applied, the post-marking image showed a highly reflecting laser cautery mark near the intended location (Figs. 12(B), (C)). White light endoscopy performed after the TCE procedure demonstrates a clearly visible laser mark on the surface of salmon-colored esophageal mucosa (Fig. 12(D), red arrow). Histology from an endoscopic

Biomedical Optics EXPRESS

biopsy obtained adjacent to the mark (Fig. 12(E)) shows specialized intestinal metaplasia, the most common form of BE.

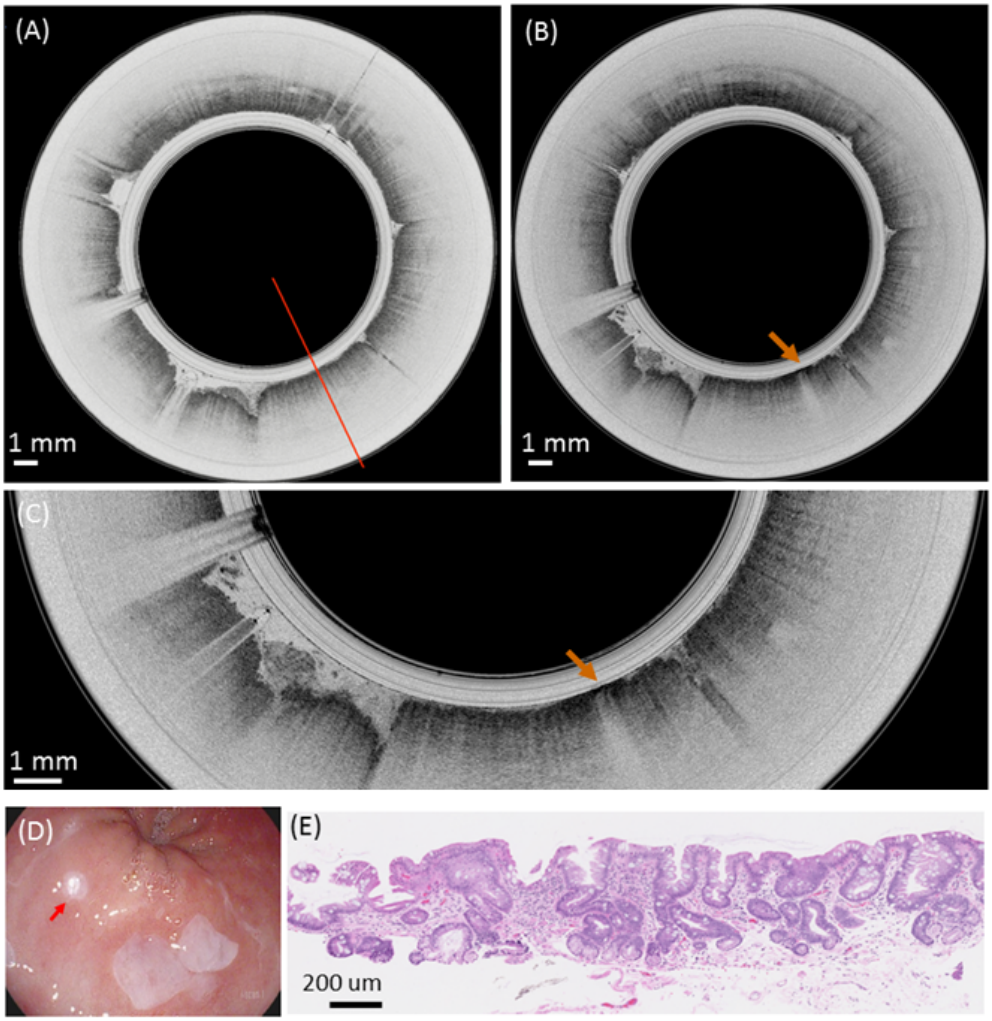

Fig. 12. TCE laser marking of Barrett's esophagus in a study subject. A) Pre-marking OCT image of BE mucosa. The red line indicates where the operator intends to place the laser marks. (B) OCT image of the study subject's esophagus after laser marking. The orange arrow points to hyper-reflective signal from the cauterized laser mark. (C) Enlarged image of the marking site, showing the OCT appearance of the laser mark (orange arrow) in greater detail. (D) Endoscopy image of the laser mark (red arrow). (E) Histology from the biopsy taken adjacent to the laser mark, confirming that the marked tissue was BE.

3.4 The accuracy of TCE laser marking in vivo

We were able to successfully co-register 9 pre- and post-marking images from the 5 subjects. After subtracting intent-to-mark and post-marking locations, the cross-sectional difference between the intended target and the actual marking positions was 0.95 +/– 0.53 (standard deviation) mm.

4. Discussion

The field of TCE is growing with many studies now using tethered capsules for GI tract diagnosis [1,2,7]. Since TCE does not have biopsy capability, it is essential that new

Biomedical Optics EXPRESS

technology become available to allow TCE images to be correlated to histopathology. Without histopathologic validation, this promising technology cannot be used for patient care. Laser marking using a tethered capsule is the most attractive way to conduct these validation studies and thus TCE laser marking technology presented in this study is a critical advancement. Moreover, we have demonstrated that using TCE laser marking to guide biopsy is feasible and safe in human subjects. After validation, the TCE device can be used independently for screening unsedated patients and for placing marks at lesions that may require follow-up during a subsequent endoscopy.

The main challenge that we encountered when conducting TCE-based laser marking was marking precision artifacts caused by motion of the capsule in the esophagus, which is greater than that of balloon-catheter VLE. By increasing the power to 800 mW and decreasing the laser exposure time to 1 second, we found that these artifacts can be overcome to produce tightly localized marks on the esophagus in living human subjects (Fig. 11(D) and 12(D)). Besides shortening the laser exposure time, we further mitigated this potential issue by performing laser marking only during pullback (Fig. 6). This procedural step allows us to fix the proximal end of the capsule to the leading edge of the peristaltic contraction. In addition, the size of targets, such as BE, dysplasia and adenocarcinoma are typically > few mm [17] and the accuracy of endoscopic biopsy is > 1 mm, which are roughly on the same scale as the ~1mm marking error at the dynamic gastroesophageal junction (GEJ) as shown in Fig. 12(A) and (B). Our overall cross-sectional targeting accuracy is 0.95 ± 0.53 mm (standard deviation from 5 subjects, 9 marks). Finally, since the hyper-reflective laser marks can be visualized in OCT images, we can correlate histology with post-marking OCT images for validating the diagnostic accuracy against histology. Given these considerations, the accuracy of TCE laser marking should be more than sufficient for most regions of interest in the esophagus.

In addition to optimizing the laser marking exposure parameters, we improved the device by incorporating a distal stepper micromotor in the capsule to scan the OCT beam. The A-line clock was used for synchronizing the A-line acquisition and motor rotation, so that a stationary target would not rotate and would remain stationary in the imaging window for high-precision marking. Once receiving the coordinate of target, the motor stopped at one of the 40 dwelling points that was closest to the target. The maximum discrepancy between the intended position and the actual dwelling position was half of the space interval between two neighboring dwelling points. Figure 10 shows the histogram of the size of space intervals. The maximum interval at the capsule's surface was 1 mm. Therefore, the maximum discrepancy between the intended position and the actual dwelling position (targeting error) was ~0.5 mm. Under same number of steps, the targeting accuracy scales inversely with diameter, as the diameter goes up, the accuracy goes down and vice versa. We have initially used 11-mm-diameter TCE devices as this is a standard set forth by predicate devices such as video capsule endoscopes. Unsedated TCE targeting accuracy is similar to sedated VLE targeting accuracy and thus both technologies may be used to guide targeted biopsy acquisition. The aim of this study was to demonstrate the feasibility of performing laser marking on unseated patients with TCE devices. In addition, since the stepper motor does not require an encoder for absolute position determination, the device can be less expensive and complex, which is consistent with the low-cost requirement of a capsule-based screening technology.

We used *ex vivo* animals to test our marking laser parameter set and froze those parameters for the clinical product. All subjects were tested under the same parameters. These parameters and the described clinical device satisfy the requirements for effective TCE-based laser marking in human subjects. For our exposure parameters (800 mW, 1430/1450 nm), the deposited laser energy, as determined by exposure duration (1-4 s), diffused predominantly in the lateral direction. From 1 to 4 seconds, the lateral injury width (Fig. 8(A)) increased by a factor of two, but the depth (Fig. 8(B)) only increased by ~20%. Therefore, it is not surprising that the laser thermal injury does not penetrate beyond muscularis mucosae even with a 4s

Biomedical Optics EXPRESS

exposure time (Fig. 8(C)). The extent of injury on the swine esophagus is comparable to that of standard biopsy forceps. For minimizing the motion artifact, we used a 1 s exposure time, which has a large 4x safety margin.

Results obtained in 5 subjects so far demonstrate that TCE laser marking can be a safe and effective way to correlate OCT TCE images to co-localized biopsies and corresponding histology. The missing mark (1 out of 12 attempts) was successfully identified in OCT image, but could not be identified by video endoscopy. Due to an uneven tissue surface, video endoscopy was not able to visualize 100% of the esophagus. In the future, we can increase the number of marks per target to avoid this potential issue. The co-localization capability is highly important now to validate the diagnosis of TCE images in histopathologic correlative studies. In addition, guided biopsy via TCE could also find similar utility to real-time targeting in VLE, enabling the sampling of aberrant tissue that is missed by random endoscopic biopsy, the current standard of care. TCE laser marking has advantages over balloon-based VLE targeting as the former can be conducted in unsedated patients at the point of care. Larger clinical studies using TCE laser marking should be conducted to validate TCE and determine its clinical utility for guiding biopsy.

Looking towards the future, it is also possible to consider a scheme where TCE diagnosis, targeting, and laser marking are performed automatically, based on advanced signal processing [18,19] or machine learning methods [20]. Such an advance could be facilitated by use of a pulsed Raman fiber laser [21], coupled into the inner cladding of a double clad fiber, recently demonstrated for ablating tissue in real time while OCT imaging [22]. This strategy would also be consistent with the screening case use scenario of tethered capsule technologies, obviating expert image interpretation during the TCE procedure.

5. Conclusion

OCT-based tethered capsule endomicroscopy is an up and coming, minimally-invasive technique for upper GI tract microscopic screening in unsedated patients. Histologic validation is a critical step that is required for the adoption of TCE. Here, we have described a TCE laser marking system and a stepper micromotor, beam scanning capsule that allows TCE OCT images to be correlated to endoscopic biopsies taken from the patient. Animal and human data using this technology in vivo shows that TCE laser marking is an effective and safe method for making this correspondence. Beyond histopathologic validation, TCE laser marking also has the potential to become a useful tool for marking microscopically abnormal tissue found during an outpatient capsule screening procedure that can subsequently be biopsied endoscopically. The convenience and cost-profile of such a strategy could significantly improve the care of patients with BE and other gastrointestinal diseases.

Funding

National Institutes of Health grants (NIH R01CA184102, R01DK100569, R01EB022077); Remondi Family Foundation; the Mike and Sue Hazard Family; the MGH Research Scholars Program.

Disclosures

Massachusetts General Hospital has a licensing arrangement with NinePoint Medical. Dr. Tearney has the rights to receive royalties from this licensing arrangement. Dr. Tearney also consults for NinePoint Medical. Dr. Tearney receives sponsored research from Boston Scientific and iLumen Medical.

References

1. M. J. Gora, J. S. Sauk, R. W. Carruth, K. A. Gallagher, M. J. Suter, N. S. Nishioka, L. E. Kava, M. Rosenberg, B. E. Bouma, and G. J. Tearney, "Tethered capsule endomicroscopy enables less invasive imaging of gastrointestinal tract microstructure," Nat. Med. **19**(2), 238–240 (2013).

Biomedical Optics EXPRESS

2. K. Liang, O. O. Ahsen, H. C. Lee, Z. Wang, B. M. Potsaid, M. Figueiredo, V. Jayaraman, A. E. Cable, Q. Huang, H. Mashimo, and J. G. Fujimoto, "Volumetric Mapping of Barrett's Esophagus and Dysplasia With en face Optical Coherence Tomography Tethered Capsule," Am. J. Gastroenterol. **111**(11), 1664–1666 (2016).
3. M. J. Gora, L. H. Simmons, L. Quénéhervé, C. N. Grant, R. W. Carruth, W. Lu, A. Tiernan, J. Dong, B. Walker-Corkery, A. Soomro, M. Rosenberg, J. P. Metlay, and G. J. Tearney, "Tethered capsule endomicroscopy: from bench to bedside at a primary care practice," J. Biomed. Opt. **21**(10), 104001 (2016).
4. M. J. Gora, J. S. Sauk, R. W. Carruth, W. Lu, D. T. Carlton, A. Soomro, M. Rosenberg, N. S. Nishioka, and G. J. Tearney, "Imaging the upper gastrointestinal tract in unsedated patients using tethered capsule endomicroscopy," Gastroenterology **145**(4), 723–725 (2013).
5. K. Liang, Z. Wang, O. O. Ahsen, H.-C. Lee, B. M. Potsaid, V. Jayaraman, A. Cable, H. Mashimo, X. Li, and J. G. Fujimoto, "Cycloid scanning for wide field optical coherence tomography endomicroscopy and angiography *in vivo*," Optica **5**(1), 36–43 (2018).
6. O. O. Ahsen, K. Liang, H. C. Lee, M. G. Giacomelli, Z. Wang, B. Potsaid, M. Figueiredo, Q. Huang, V. Jayaraman, J. G. Fujimoto, and H. Mashimo, "Assessment of Barrett's esophagus and dysplasia with ultrahigh-speed volumetric en face and cross-sectional optical coherence tomography," Endoscopy (to be published).
7. K. Li, W. Liang, J. Mavadia-Shukla, H. C. Park, D. Li, W. Yuan, S. Wan, and X. Li, "Super-achromatic optical coherence tomography capsule for ultrahigh-resolution imaging of esophagus," J. Biophotonics doc. ID e201800205 (posted 8 October 2018, in press).
8. M. J. Gora, L. Quénéhervé, R. W. Carruth, W. Lu, M. Rosenberg, J. S. Sauk, A. Fasano, G. Y. Lauwers, N. S. Nishioka, and G. J. Tearney, "Tethered capsule endomicroscopy for microscopic imaging of the esophagus, stomach, and duodenum without sedation in humans (with video)," Gastrointest. Endosc. **88**(5), 830–840 (2018).
9. A. S. O. P. Committee, J. A. Evans, D. S. Early, N. Fukami, T. Ben-Menachem, V. Chandrasekhara, K. V. Chathadi, G. A. Decker, R. D. Fanelli, D. A. Fisher, K. Q. Foley, J. H. Hwang, R. Jain, T. L. Jue, K. M. Khan, J. Lightdale, P. M. Malpas, J. T. Maple, S. F. Pasha, J. R. Saltzman, R. N. Sharaf, A. Shergill, J. A. Dominitz, B. D. Cash, and E. Standards of Practice Committee of the American Society for Gastrointestinal, "The role of endoscopy in Barrett's esophagus and other premalignant conditions of the esophagus," Gastrointest. Endosc. **76**(6), 1087–1094 (2012).
10. M. J. Suter, B. J. Vakoc, P. S. Yachimski, M. Shishkov, G. Y. Lauwers, M. Mino-Kenudson, B. E. Bouma, N. S. Nishioka, and G. J. Tearney, "Comprehensive microscopy of the esophagus in human patients with optical frequency domain imaging," Gastrointest. Endosc. **68**(4), 745–753 (2008).
11. H. C. Wolfsen, P. Sharma, M. B. Wallace, C. Leggett, G. Tearney, and K. K. Wang, "Safety and feasibility of volumetric laser endomicroscopy in patients with Barrett's esophagus (with videos)," Gastrointest. Endosc. **82**(4), 631–640 (2015).
12. M. J. Suter, M. J. Gora, G. Y. Lauwers, T. Arnason, J. Sauk, K. A. Gallagher, L. Kava, K. M. Tan, A. R. Soomro, T. P. Gallagher, J. A. Gardecki, B. E. Bouma, M. Rosenberg, N. S. Nishioka, and G. J. Tearney, "Esophageal-guided biopsy with volumetric laser endomicroscopy and laser cautery marking: a pilot clinical study," Gastrointest. Endosc. **79**(6), 886–896 (2014).
13. A. F. Swager, A. J. de Groof, S. L. Meijer, B. L. Weusten, W. L. Curvers, and J. J. Bergman, "Feasibility of laser marking in Barrett's esophagus with volumetric laser endomicroscopy: first-in-man pilot study," Gastrointest. Endosc. **86**(3), 464–472 (2017).
14. M. Alshelleh, S. Inamdar, M. McKinley, M. Stewart, J. S. Novak, R. E. Greenberg, K. Sultan, B. Devito, M. Cheung, M. A. Cerulli, L. S. Miller, D. V. Sejpal, A. K. Vegesna, and A. J. Trindade, "Incremental yield of dysplasia detection in Barrett's esophagus using volumetric laser endomicroscopy with and without laser marking compared with a standardized random biopsy protocol," Gastrointest. Endosc. **88**(1), 35–42 (2018).
15. K. Liang, G. Traverso, H. C. Lee, O. O. Ahsen, Z. Wang, B. Potsaid, M. Giacomelli, V. Jayaraman, R. Barman, A. Cable, H. Mashimo, R. Langer, and J. G. Fujimoto, "Ultrahigh speed en face OCT capsule for endoscopic imaging," Biomed. Opt. Express **6**(4), 1146–1163 (2015).
16. M. J. Suter, P. A. Jillella, B. J. Vakoc, E. F. Halpern, M. Mino-Kenudson, G. Y. Lauwers, B. E. Bouma, N. S. Nishioka, and G. J. Tearney, "Image-guided biopsy in the esophagus through comprehensive optical frequency domain imaging and laser marking: a study in living swine," Gastrointest. Endosc. **71**(2), 346–353 (2010).
17. A. J. Cameron and H. A. Carpenter, "Barrett's esophagus, high-grade dysplasia, and early adenocarcinoma: a pathological study," Am. J. Gastroenterol. **92**(4), 586–591 (1997).
18. A. F. Swager, D. J. Faber, D. M. de Bruin, B. L. Weusten, S. L. Meijer, J. J. Bergman, W. L. Curvers, and T. G. van Leeuwen, "Quantitative attenuation analysis for identification of early Barrett's neoplasia in volumetric laser endomicroscopy," J. Biomed. Opt. **22**(8), 086001 (2017).
19. G. J. Ughi, M. J. Gora, A. F. Swager, A. Soomro, C. Grant, A. Tiernan, M. Rosenberg, J. S. Sauk, N. S. Nishioka, and G. J. Tearney, "Automated segmentation and characterization of esophageal wall in vivo by tethered capsule optical coherence tomography endomicroscopy," Biomed. Opt. Express **7**(2), 409–419 (2016).
20. T. H. Tsai, C. L. Leggett, A. J. Trindade, A. Sethi, A. F. Swager, V. Joshi, J. J. Bergman, H. Mashimo, N. S. Nishioka, and E. Namati, "Optical coherence tomography in gastroenterology: a review and future outlook," J. Biomed. Opt. **22**(12), 1–17 (2017).
21. H. W. Baac, N. Uribe-Patarroyo, and B. E. Bouma, "High-energy pulsed Raman fiber laser for biological tissue coagulation," Opt. Express **22**(6), 7113–7123 (2014).

Biomedical Optics EXPRESS

22. K. Beaudette, H. W. Baac, W. J. Madore, M. Villiger, N. Godbout, B. E. Bouma, and C. Boudoux, "Laser tissue coagulation and concurrent optical coherence tomography through a double-clad fiber coupler," Biomed. Opt. Express **6**(4), 1293–1303 (2015).